Electrochemical oxydation of vanadyl ions in phosphorique acid solution

M. El Joumani*, S. Bououd, Z. El Abbassi, F. Saidi, A. Kafih, , A. El Hourch*, A. Guessous

Electrochemistry and analytical chemistry team, Department of Chemistry, Faculty of Science,
Mohammed V University in Rabat, Morocco.

Abstract

The oxidation of vanadyl ions in phosphoric acid led to the formation and well crystallization of deposit. By means of the voltammetry cyclic, we were able to show the mechanism of the formation of the electrolytic deposit by diffusion. The study of the influence of certain parameters such as the potential of electrolysis, the concentration of vanadyl ions and phosphoric acid H_3PO_4, the scanning rates and the medium pH in particular, was realized. The irreversible behavior was shown. The charge transfer coefficient and the ion diffusion coefficient of vanadyl ions were calculated.

Key words: voltammetry, vanadium, deposit, diffusion

Introduction

Li-ion rechargeable batteries have advantages of high power density and good reversibility compared to other types of rechargeable batteries. Among the various compounds containing Li metal phosphates have been attracting much interest as new cathode materials for Li-ion rechargeable batteries [1–5]. This is because metal phosphates are generally more stable than oxides and some of them have unique layered and/or tunnel structures. In fact, its preparation by generally ''high temperature'' methods induces the sintering and aggregation of particles, which are deleterious for its electrochemical performance. It was found that lowering the sintering temperature and/or adding conductive particles to $LiMPO_4$ remarkably improved the capacity of the material as a consequence of diminished particle size [6-10]. Cathode materials are beginning to be prepared at low temperatures using aqueous solution systems [11]. They include, precipitation methods, sol–gel process, and hydrothermal techniques, which provide intimate mixing of the component elements in the solution allowing finer particles and high-purity materials to be produced by rapid homogeneous nucleation [12-15]. Electrochemical methods for the fabrication of a thin film have many advantages over other methods in terms of economics and flexibility. Electrodeposition is carried out at low temperatures. A thin film can be fabricated on the surface of the electrode, which is formed by the electrochemical potential. A porous structure can be controlled by varying the electrodeposition conditions, such as deposition voltage, deposition time and surfactant concentration. The electrode is synthesized directly without a binding or pasting process. The surfactant can be removed easily by washing with an appropriate solvent. The electrolytic V_2O_5 was prepared by electrochemical oxidation of vanadyl ions in aqueous solutions with H_2SO_4 or HCl as the electrolyte [16-19]. Potiron et al. [18] reported that poorly crystallized mixed-valence compounds corresponding to $V_2O_{5-n/2}$, nH_2O formula were obtained. Vanadyl phosphates ($VOPO_4$) represent a class of attractive cathodes in lithium-ion batteries. However, the exploration of this type of materials in sodium-ion batteries is rare. Here, we report for the first time a mechanism of the synthesis of orthorhombic $Na_{0.45}VOPO_4$, $1.58H_2O$ [20]. The ubiquitous availability of inexpensive sodium and the increasing demand for lithium used in Li-ion batteries has prompted investigation of Na-ion batteries based on chemical strategies similar to those used for rechargeable Li-ion batteries [21-23]. In this study the mechanism of potentiostatic deposition of $Na_{0.45}VOPO_4$, $1.58H_2O$ has been investigated by using cyclic voltammetry.

2. Materials and methods

All electrochemical experiments were carried out using a conventional set up comprising a three-electrode electrochemical cell connected to a computer-controlled Radiometer Analytical PGZ 301 potentiostat-galvanostat. The three-electrode electrochemical cell was placed in a double jacket to maintain a constant temperature throughout the experiment by circulation of thermo-stated water, i. e. 25°C or 70°C. The working electrode was a $1cm^2$ Pt plate. A saturated calomel electrode (SCE) was used as the reference electrode and the counter electrode was a wide-area Pt grid.

Just prior to the deposition, the working electrode were polished using different grades of Al_2O_3 powder. The electrodes were rinsed with ultrapure water (18 $M\Omega.cm^{-1}$) and were placed in solutions comprising of vanadyl sulfate $VOSO_4$ (0,1M) in phosphoric acid (H_3PO_4 (1M)). The purity of the phosphoric acid is 85%. Several series of experiments corresponding to solutions with different pH were carried out.

The solution was stirred throughout the experiment. Applied voltage is 1.5V/SCE and the sweep rate is 100 mVs^{-1}.Green deposits resulting from the electrochemical oxidation of vanadyl sulfate were collected at the working electrode, washed with distilled water and then dried for several hours in air.

3. Results and discussion

3.1. Influence of pH

The pH was the first parameter which influence was studied since it is a crucial parameter in the occurring reaction. Figures 1 and 2 shows the repetitive voltamograms (30 cycle) of vanadyl solution (0,1M) in H_3PO_4 (1M) the NaOH was used to adjust the pH for two solutions, one with pH= 1.4, the second one with pH= 2. At pH= 1.4 we observe the oxidation of vanadyl V^{4+} to V^{5+} at the reverse scan, we observe the reduction of vanadium V to vanadium IV.
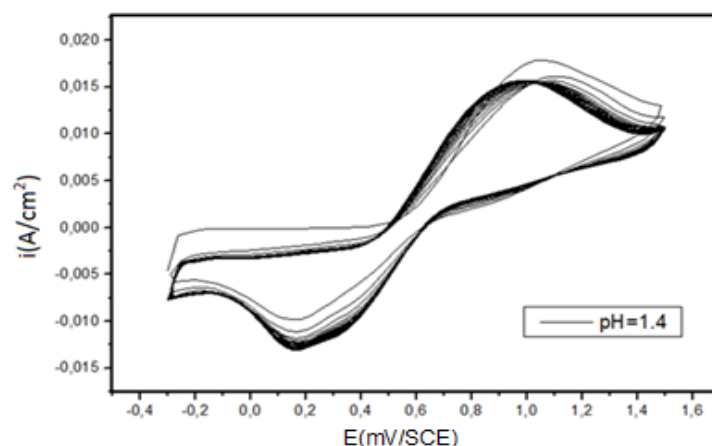

Figure 1: Repetitive cyclic voltammograms of 0.1M $VOSO_4$ + 1M H_3PO_4 + NaOH (pH 1.4). Sweep rate, $100mVs^{-1}$.
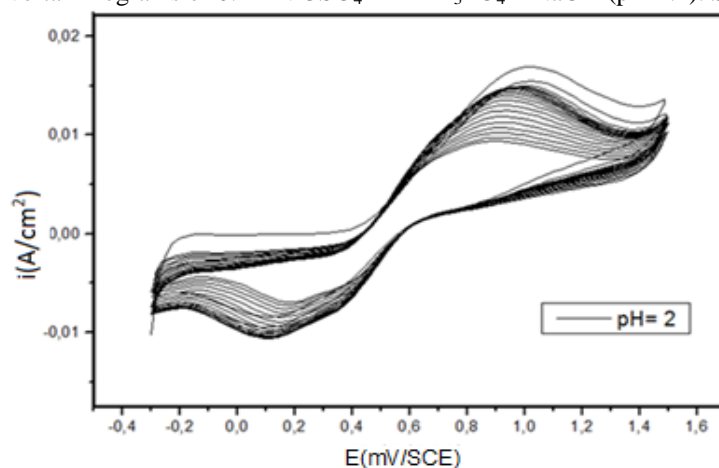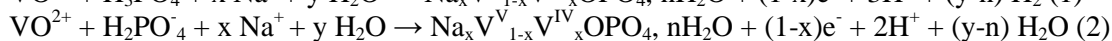

Figure 2: Repetitive cyclic voltammograms of 0.1M $VOSO_4$ +1M H_3PO_4 + NaOH (pH= 2). Sweep rate, 100 mVs^{-1}.

The intensitys of the peaks, is almost inchanged, during cycling that either for oxidation or reduction. Unlike pH=2, with a huge and clear deference, the intensity of the peaks of oxidation and reduction decreases during cycling. Because the concentration in vanadyl ion within the solution decreases during cycling and the surface of the electrode decrease in case of oxidation to match 1,05 V and shifts to more negative potential , in this case the green thin film appeared at the surface of the electrode . The X-ray diffraction pattern of the material obtained at pH 2 is given in Fig. 3a. All the diffraction peaks in the pattern are in agreement with those of $Na_{0.45}VOPO_4$, $1.58H_2O$ [file JCP 05 00-041-0087][24]. No characteristic peaks of impurity phases are present, indicating the high purity of the samples. The material is an orthorhombic phase with lattice parameters a =8.85 Å, b = 9.01 Å and c =13.02 Å. A SEM image of the deposit is shown in Figure 3 porous structure is observed.

Owing to the pH of the solution being 2 and according to [25], The oxidation of the vanadyl ions produces $HnV_{10}O_{28}^{(6-n)-}$ with n depending on pH. The precipitation would then be favored by the presence of protons produced by water oxidation on the electrode surface and the resulting decrease in local pH at the surface or in the vicinity of the electrode [26]. The presence of $H_2PO_4^-$ is due to the use of H_3PO_4 as electrolyte and finally the presence of Na^+ ions is due to the use of NaOH to adjust the pH. It would occur according to equations (1) and (2). The guest Na^+ ions are located in the inter-lamellar space and the deposit obtained contains a mixed IV/V vanadium oxidation.

$$VO^{2+} + H_3PO_4 + x\ Na^+ + y\ H_2O \rightarrow Na_xV^V_{1-x}V^{IV}_xOPO_4, nH_2O + (1-x)e^- + 3H^+ + (y-n)\ H_2\ (1)$$

$$VO^{2+} + H_2PO^-_4 + x\ Na^+ + y\ H_2O \rightarrow Na_xV^V_{1-x}V^{IV}_xOPO_4, nH_2O + (1-x)e^- + 2H^+ + (y-n)\ H_2O\ (2)$$

On the basis of the above data, it appeared that deposits onto the Pt electrode could be obtained for E >1.1 V/ECS and for solutions with pH≥2 in phosphoric acid solutions.
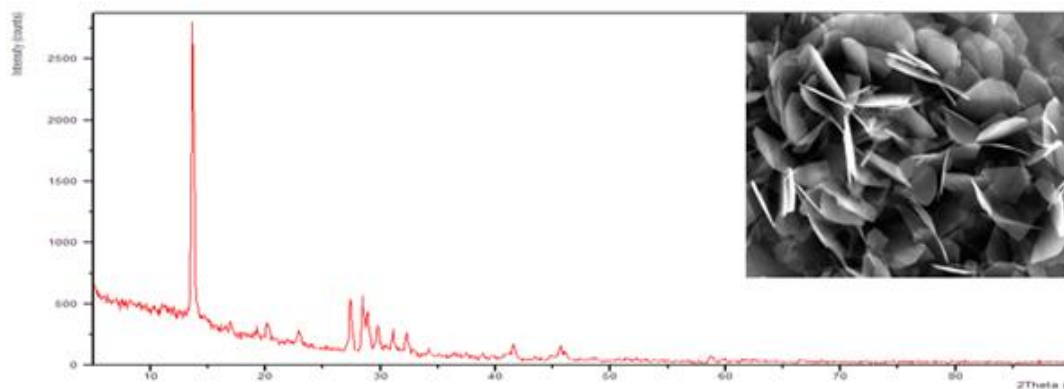
Figure 3: X-ray diffraction of the deposit obtained for solution comprising 0.1 mol L^{-1} of vanadyl sulfate (VOSO$_4$) in phosphoric acid (H$_3$PO$_4$ 1 mol L^{-1}) at pH = 2. The inset is the corresponding SEM image of the deposit

3.2. Influence of the anodic limits
Cyclic voltammograms of 0.1M VOSO$_4$ + 1M H$_3$PO$_4$ solution, show significant differences when the anodic limits were changed from 0.2 to 1.5V (Figure. 4).
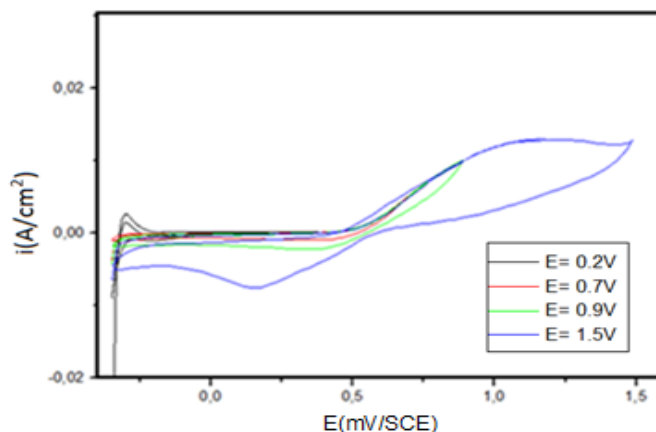

Figure 4: Cyclic voltammograms of 0,1M VOSO$_4$ in 1M H$_3$PO$_4$, anodic limits, Sweep rate, 100 mVs^{-1}.

Where the anodic limit was 0.2, 0.7 and 0.9V, non deposit was detected on surface of Pt. A positive limit of 1.05V was required for vanadophosphate deposition. The anodic limit dependence is explained taking into account the water discharge reaction (WDR).

Potentials higher than 1,05 V are required to oxidize V^{IV} to V^V, and the oxidation of water occurs concomitantly at these potential clearly suggest that the oxidation of water must occurs for vanadophosphate electrodeposition [20].

*3.3. Influence of the concentration of vanadyl*

Various vanadyl concentration solutions, from 0.01M to 0.2M, were used for voltammetry experiments. Figure. 5 shows the potentiodynamic curve obtained in these solutions. The density of the anodic peak current increase with increasing VO^{2+} concentrations.
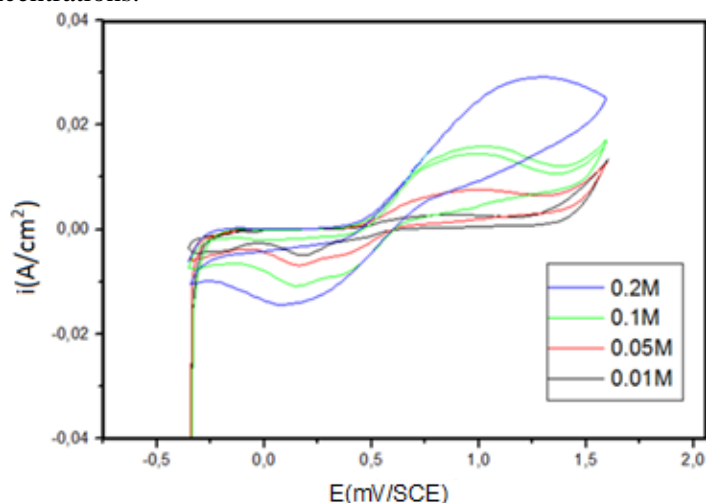
Figure 5: Cyclic voltammograms for different concentrations of VO^{2+} in 1M H_3PO_4 at a scan rate of 100 mV s^{-1}

Cyclic voltammograms for different concentrations of VO^{2+} solutions on Pt electrode at a scan rate of 0,1V.s^{-1} (Figure. 5) exhibited an anodic peak around 1.05 V which increased in height and shifted slightly towards more positive potentials with increasing VO^{2+} concentration. At higher concentration, the anodic peak appeared at a more positive potential of~1.1V. However, the cathodic peak at ~0.15V was found to be roughly 10 times smaller than the anodic one.

The peak current increased with VO^{2+} concentration showing a small negative deviation from linearity while the peak potential shifted to more positive values (Figure. 6). The anodic peak observed at considerably more positive potential (~1.1V) for higher concentration of VO^{2+} ions increasing VO^{2+} concentration, indicates the generation of still higher oxidation state of V(IV) to V(V).
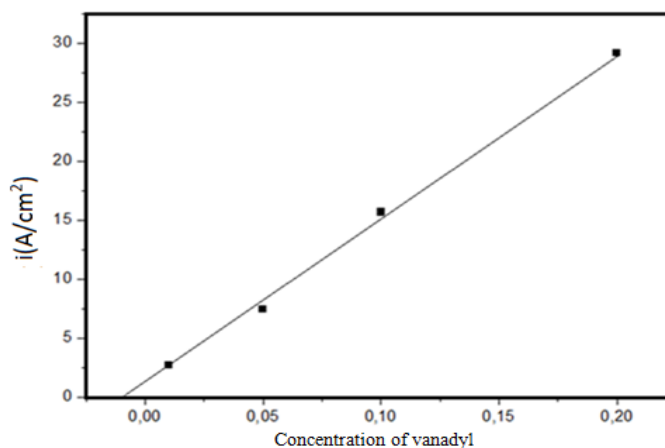
Figure 6: anodic peak current density (i_p) vs. [VO^{2+}] in 1M H_3PO_4.

3.4. The relationship between the peak current and the scan rate.

Various scanning rates from 20 mV/s to 400 mV/s, were used for voltammetry experiments. Figure. 7 shows the potentiodynamic curve obtained in these solutions. Anodic peak current density increase with increasing the scanning rates
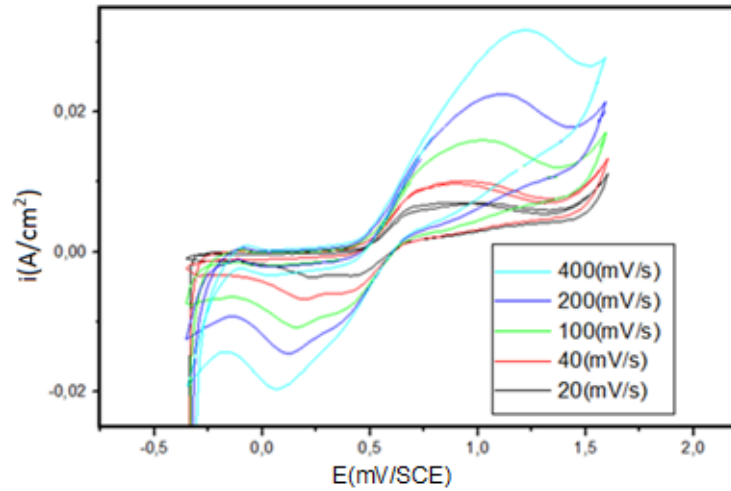

**Figure7**: Cyclic voltammograms of the as-prepared $Na_{0.45}VOPO_4$, $1.58H_2O$ at different scan rates.

Table 2: Anodic and cathodic peak current densities (i_p) at different potential scan rates.

v (V/s)	0.02	0.04	0.1	0.2	0.4
$v^{1/2}(V/s)^{1/2}$	0.14	0.2	0.3	0.44	0.63
$i_{pa}(A/cm^2)$	0.006	0.009	0.015	0.022	0.031
$i_{pc}(A/cm^2)$	-0.003	-0.006	-0.01	-0.014	-0.019
$E_{pa}(V)$	0.85	0.91	0.96	1.11	1.21
$E_{pc}(V)$	0.24	0.19	0.15	0.11	0.064

On the other hand, much smaller cathodic peak, compared to the anodic one, obtained during the reverse sweep and observed. The observed linear variation of anodic peak current (ip_a) with square root of potential scan rate (v) at fixed VO^{2+} concentration (Fig.7) indicates that the rate-determining step is the diffusion of VO^{2+}ions.
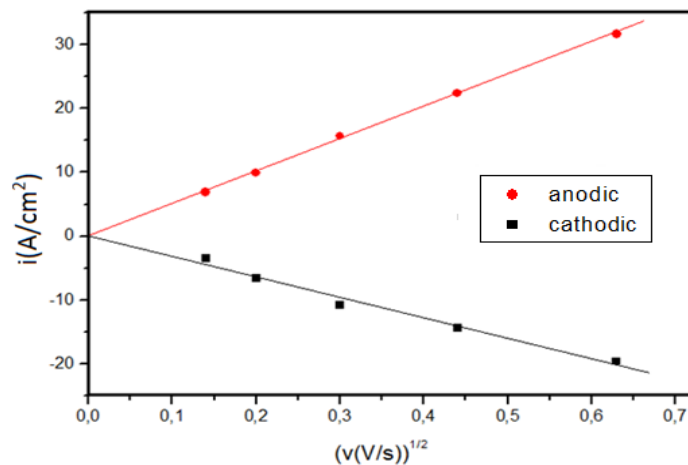
Figure 8: anodic and cathodic peaks current densitys (i_{pa}) vs.$V^{1/2}$ for 0.1 M $VOSO_4$ in 1M H_3PO_4.
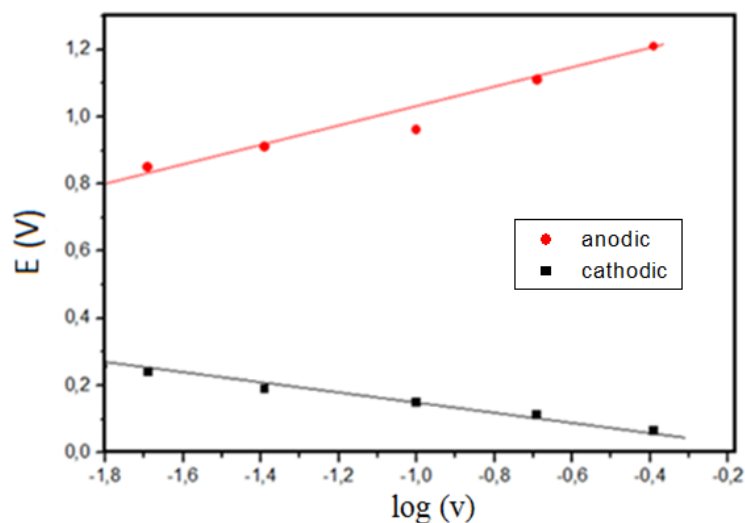
Figure 9: Peaks potential cathodic and anodic versus log (v) for 0,1 M $VOSO_4$ in 1M H_3PO_4.

In fig. 7 and table 2 we observe when the scan rate was increased, the cathodic and anodic peaks moved to lower and higher potentials, respectively, and the peak intensity increased. The difference in the potential of the anodic peak and that of their corresponding cathodic peaks became larger with the increase in the scan rate. This was further evidence of the irreversible nature of the electrochemical reactions. Moreover, the integral area of redox peaks increases with increasing the scan rate, which may be attributed to the direct proportion of peak area to the scan rate [27] as shown in figure. 8 each redox peak current (i_p) has a linear relationship with the square root of scan rate ($v^{1/2}$), and the equation for a semi in finite diffusion of vanadyl into cathode can be applied:

$$I_p = (2.99 \times 10^5) \times n(\alpha n)^{1/2} \times A \times D^{1/2} \times C \times v^{1/2}$$

The peak potential was found to be dependent of log v, indicating the poor reversibility of the system (Figure.9) The numerical constant corresponds to expressing I_p is the peak current (A); A is the surface area of the electrode (cm^2); D is the diffusion coefficient of the vanadium ion ($cm^2.s^{-1}$); C is the concentration of vanadium ($mol.cm^{-3}$); V is the scanning rate ($V.s^{-1}$); n is the number of electrons transferred in the electrode reaction. In this paper, n is equal to 1 and α is the coefficient of charge transfer for an irreversible system. The expression of potential for this system is [28]:

$E = E^{o'} - \frac{RT}{\alpha nF}[0.780 + Ln(\frac{D}{K}) + ln(\frac{\alpha nFv}{RT})^{1/2}]$

Where $2.3\frac{RT}{2\alpha nF}$ is the slope of E vs log(v) plot. $2.3\frac{RT}{2\alpha nF} = 0.28$

R= Constant of perfect gas 8.32 J deg^{-1}k

T: temperature in K

F : Number of faraday (96500)

Then α= 0.1

The diffusion coefficient (D) was calculated from the of I_{pa} vs. $v^{1/2}$ giving a value of:

D= 2.79×10^{-7} cm^2 s^{-1}; the value is comparable to that found in the electrodeposition process of V_2O_5 deposit [29].

Conclusion

In this paper, we have studied the mechanism of oxidation of vanadyl ions in phosphoric acid diluted in pH=2. We were able to show that the oxidation is governed by diffusion process. The irreversible behavior was shown. The charge transfer coefficient is on the order 0.1 and the ion diffusion coefficient of vanadyl is the order 2.79×10^{-7} cm^2 s^{-1}. This work illustrates a route for the fabrication of high quality of crystalline $Na_{0.45}VOPO_4$, $1.58H_2O$ by electrodeposition process using an aqueous solution of vanadyl ions in phosphoric acid.

Reference

1. Padhi K., *J. Electrochem. Soc.* 144 (1997) 1188.
2. Ellis B., Wang Hay Kan., Makahnouk W. R. M., Nazar L. F., *J. Mater. Chem*. 17 (2007) 3248–3254.
3. Dominko R., Bele M., Gaberscek M., Remskar M., Hanzel D., Pejovnik S., Jamnik. J., J. *Electrochem. Soc.* 152 (2005) A607-A610.
4. Huang H., Yin S C., Nazar L.F., *Electrochem. Solid-State Lett*. 4 (2001) a170-a172.
5. Chung S.Y., Bloking J.T., Chiang Y.M., *Nat. Mater.*1 (2002) 123-128.
6. Zhumabay B., Izumi T., *Electrochem. Commun.* 12 (2010) 75–78.
7. Daiwon C., Donghai W., In-Tae B., Jie X., Zimin N., Wei W., Vilayanur V. Viswanathan., Yun Jung L., Ji-Guang Z., Gordon L. G., Zhenguo Y., Jun L*., Nano Lett.* 10 (2010) 2799–2805.
8. Delacourt C., Poizot. P., Morcrette. M., Tarascon. J. M., Masquelier. C., *Chem. Mater*. 16 (2004) 93-99.
9. Takayuki D., Shota Y., Tetsuya K., Shigeto O., Jun-ichi Y., *Cryst. Growth Des*. 9(2009) 4990-4992.
10. Kim T. R., Kim D. H., Ryu H.W., Moon J.H., Lee J.H., Boo S., Kim J., *Phys. J. Chem. Solids*. 68 (2007) 1203-1206.
11. Wang D., Buqa H., Crouet M., Deghenghi G., Dreen T., Exnar I., Kwon N.-H., Miners J.H., Poletto L., Graetzel M., *J. Power Sources*, 189 (2009) 624-628.
12. Haisheng F., Liping Li., Yong Y., Guofeng Y., Guangshe Li., *Chem. Commun*.(2008) 1118-1120.
13. Yuan W., Yan J., Tang Z.Y., Ma L., *Ionics* 18 (2012)329.
14. Dokko K., Koizumi S., Nakano H., Kanamura K., *J Mater. Chem*. 17 (2007) 4803.
15. Sun C.W., Rajasekhara S., Dong Y.Z., Goodenough J.B., *ACS Appl. Mater. Inter*. 3 (2011) 3772.
16. E. Deltombe, N. de Zoubov, M. Pourbaix, in: Gauthiais eVillars (Ed.), *Atlas d'Equilibre Electrochimiques* (1963), pp. 234e235
17. Potiron E., La Salle A. L., Verbaere. A., Piffard. Y., Guyomard. D., *Electrochim. Acta* 45 (1999) 197.
18. Potiron E., Sarciaux S., Piffard Y., Guyomard D., *J. Power Sources* 81-82(1999) 666.
19. Sato Y., Nomura T., Tanaka H., Kobayakawa K., *J. Electrochemical. Soc*. 138 (1991) L37.
20. Bououd S., EL Hourch. A., K EL Kacemi., A Guessous., A Pradel., M Ribes,. *J. Solid State Sciences* 13 (2011) 2090-2095.
21. Palomares V., Serras P., Villaluenga I., Hueso K., Carretero-Gonzalez B., Rojo J., *Energy Environ. Sci*., 2012, 5, 5884–5901.
22. Slater M. D., Kim D., Lee E and Johnson C. S., *Adv. Funct. Mater*. 2013, 23, 947–958. 3 S.
23. Kim W., Seo D. H., Ma X. H., Ceder G and Kang K., *Adv. Energy Mater*., 2012, 2, 710–721
24. Casan N., Amoros P., Ibanez R., Martinez-Tamayo E., Beltran-Porter A., Beltran-Polter D., *J. Incl. Phenom*. 6 (1988) 193.
25. Alonso B., Livage J*., Solid State chemistry*, 148 (1999) 16-19.
26. Takahashi k., Limmer S.J., Wang Y., Cao G., *J. Phys. Chem.B*. 108 (2004) 9795.
27. Yin S.C., STrobel P.S., Grondey H., Nazar L.F., *Chemistry of Materials* 16 (2004) 1456.
28. Bard A ., Faulkner L., Rosset R., Bauer D., *book*. *Paris*. *New York*. *Masson*, 1983.
29. Armstrong E., O'Sullivan M., O'Connell J., D. Holmes J. and O'Dwyer C., *J. Electrochemical. Soc*, 162 (2015) D605-D612